JOURNAL OF combinatorial CHEMISTRY

Article

Combinatorial Materials Research Applied to the Development of New Surface Coatings X: A High-Throughput Electrochemical Impedance Spectroscopy Method for Screening Organic Coatings for Corrosion Inhibition

Jie He, James Bahr, Bret J. Chisholm, Jun Li, Zhigang Chen, Se#va N. Balbyshev, Verena Bonitz, and Gordon P. Bierwagen

J. Comb. Chem., **2008**, 10 (5), 704-713• DOI: 10.1021/cc8000458 • Publication Date (Web): 27 June 2008

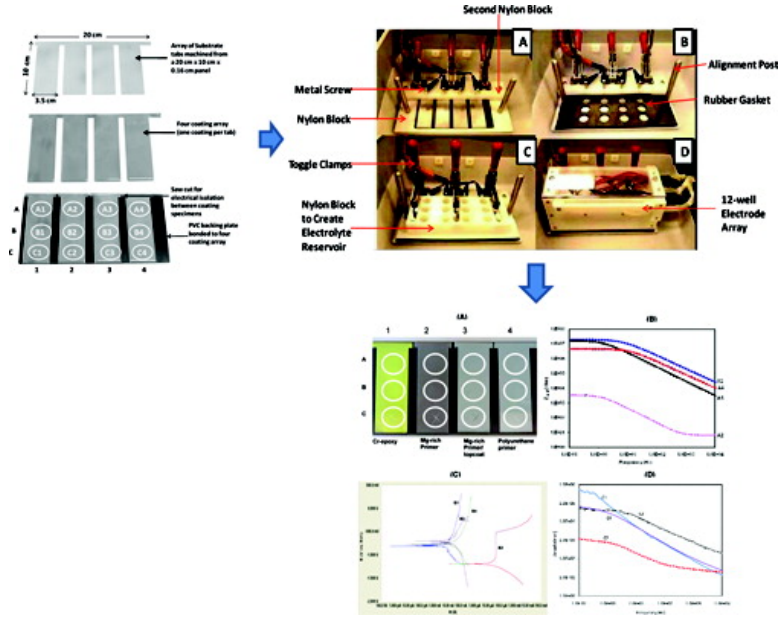

More About This Article

Additional resources and features associated with this article are available within the HTML version:

- Supporting Information
- Access to high resolution figures
- Links to articles and content related to this article
- Copyright permission to reproduce figures and/or text from this article

Journal of Combinatorial Chemistry is published by the American Chemical Society. 1155 Sixteenth Street N.W., Washington, DC 20036

Combinatorial Materials Research Applied to the Development of New Surface Coatings X: A High-Throughput Electrochemical Impedance Spectroscopy Method for Screening Organic Coatings for Corrosion Inhibition

Jie He,*,† James Bahr,† Bret J. Chisholm,†,‡ Jun Li,‡ Zhigang Chen,† Séva N. Balbyshev,† Verena Bonitz,‡ and Gordon P. Bierwagen‡

Center for Nanoscale Science and Engineering, North Dakota State University, 1805 Research Park Drive, Fargo North Dakota 58102, and, Department of Coatings and Polymeric Materials, North Dakota State University, 1735 Research Park Drive, Fargo North Dakota 58102

Received March 17, 2008

The objective of the study was to develop a high-throughput electrochemical impedance spectroscopy (HT-EIS) method for rapid and quantitative evaluation of corrosion protective coatings. A 12-element, spatially addressable electrochemical platform was designed, fabricated, and validated. This platform was interfaced to a commercial EIS instrument through an automated electronic switching unit. The HT-EIS system enables four parallel EIS measurements to be run simultaneously, which significantly reduces characterization time compared to that of serial EIS measurements using a multiplexer. The performance of the HT-EIS system was validated using a series of model systems, including a Randles equivalent circuit, an electrochemical reaction (Ti/K_4FeCN_6, K_3FeCN_6), a highly uniform polymer film, and several polymer coatings. The results of the validation studies showed that the HT-EIS system enables a major reduction in characterization time and provides high quality data comparable to data obtained with conventional, single-cell EIS measurement systems.

Introduction

Historically, the use of organic coatings has proven to be the most economical and effective method for reduction of metal corrosion. It has been reported that at least one-half of all costs for corrosion protection is related to the application and maintenance of organic surface coatings.[1,2] In recent decades, a variety of high performance coatings, such as lead-, chromate-, and tin-containing coatings, have been or will be banned as a result of stricter environmental, health, and safety regulations. Consequently, novel, environmentally benign corrosion protective coatings are needed.

Electrochemical impedance spectroscopy (EIS) has proven to be one of the most useful tools for characterizing organic coatings designed for corrosion control.[3–5] The utility of EIS arises from the electrochemical nature of the corrosion process and the relative ease of application in either a laboratory or field setting. Unlike traditional exposure methods for characterization of corrosion protection, such as ASTM B117 salt spray exposure[6] or Prohesion exposure,[7] EIS provides quantitative data in a relatively short period of time. In addition, the nondestructive nature of EIS enables repeated measurements on the same specimen, making it possible to monitor coating performance as a function of exposure time.

In recent years, the combinatorial methodology originally developed within the pharmaceutical industry has been successfully applied to coating research and development as a means to reduce the time and cost for new coating development.[8–12] High-throughput (HT) methods for preparating, depositing, curing, and testing many key properties of surface coatings have been previously described. For example, a combinatorial workflow for the development of protective coatings for plastic substrates has been described in detail by Chisholm et al.,[9] while a complete combinatorial workflow for the development of new marine coatings has been described by Webster et al.[13] A key component of a combinatorial workflow for the development of new organic coatings for corrosion control is the generation of a HT method for assessment of corrosion protection. Despite the existence of a few HT electrochemical methods reported for electrosynthesis[14,15] and screening of electrocatalysts, sensors, and batteries,[16–18] no electrochemical methods have been reported for screening of corrosion protective coatings. This document describes the design, fabrication, and validation of a HT method for assessing the corrosion protection of coatings using EIS. The device is referred to throughout this document as a HT-EIS system.

Experimental Section

Materials. Panels (20 cm × 10 cm × 1 mm) of the aluminum alloy AA 2024-T3 were obtained from Q-panel Laboratory Products (Westlake, OH). Prior to use, the panels

* To whom correspondence should be addressed. E-mail: jie.he@ndsu.edu.
† Center for Nanoscale Science and Engineering.
‡ Department of Coatings and Polymeric Materials.

10.1021/cc8000458 CCC: $40.75
Published on Web 06/27/2008

were sandblasted to remove the oxide layer and then cleaned with hexane. Panels (20 cm × 10 cm × 1 mm) of titanium were obtained from McMaster-Carr (Elmhurst, IL). A Tedlar film was obtained from DuPont (Wilmington, DE), and the film thickness was 51 μm. A silver-containing epoxy coating (Circuitworks 7100) was obtained from ITW Chemtronics (Kennesaw, GA). An epoxy adhesive, QUIK-CURE was obtained from BSI (Atascadero, CA). A two-component, chromate-based primer coating, MIL-PRF-23377J, and a two-component polyurethane topcoat, MIL-PRF-85285D, were obtained from Deft, Inc. (Irvine, CA). An epoxy resin, Epon 1001-CX-75, and an amine-functional cross-linker, Epicure 3140, were obtained from Resolution Performance Products (Houston, TX). A modified fumed silica, Aerosil R974, was obtained from Degussa GmbH (Düsseldorf, Germany). Magnesium (Mg) particles, Eckagranules PK31 and Eckagranules PK51, were obtained from Ecka GmbH (Furth, Germany). Methyl isobutyl ketone (MIBK), hexane, xylene, K_4FeCN_6, K_3FeCN_6, HF, HNO_3, and NaCl were obtained from Sigma-Aldrich Company. All chemicals were used as received from the supplier.

A Mg-rich primer coating was prepared as follows: 67 g of Epon 1001-CX-75 was dissolved in a solvent mixture composed of 45 g of MIBK and 20 g of xylene. Next, 1 g of Aerosil R974 and 95 g of a 52/48 v/v mixture of Eckagranules PK31 and Eckagranules PK51 were added to the mixture using high-shear mixing. Just prior to application of the coating to a substrate, 9.5 g of Epicure 3140 was added with stirring.

Instrumentation. For measurements made using the HT-EIS system, four femtostats of a Gamry MultiEchem 8 Electrochemical Workstation and Gamry Framework software were used to acquire impedance spectra as a function of frequency; 10 mV rms voltages vs open circuit potential were applied as the excitation signal and impedance was measured using 10 points/per decade.

For measurements made using a conventional, single-cell EIS system, sections of poly(vinyl chloride) (PVC) tubing with an inner cross-sectional area of 5 cm^2 were adhered with QUIK-CURE adhesive to the surface of sample specimens. After the adhesive was fully cured, 10 mL of electrolyte solution was poured in the open end of the tubing to create the electrolyte reservoir. Then, an Ag/AgCl reference electrode and a Pt mesh counterelectrode were placed into the solution, and the separation distance between the sample specimen and the counterelectrode was adjusted to 1.5 cm. The single cell was connected directly to a Gamry femtostat within the same Gamry MultiEchem 8 Electrochemical Workstation used for measurements with the HT-EIS system. All data fitting described in this document was conducted using Zview software from Scribner Associates.

Randles Circuit Calibration and Open-Lead Experiment. The Randles equivalent circuit[19] is one of the simplest and most common circuit models for EIS measurements. Thus, four equivalent Randles circuits (Gamry, Inc.) were used for circuit calibration experiments (Figure 1). Each circuit was connected through its respective electronic switch to its respective cell in the 12-well assembly of the HT-EIS system, and the EIS experiments were run simultaneously.

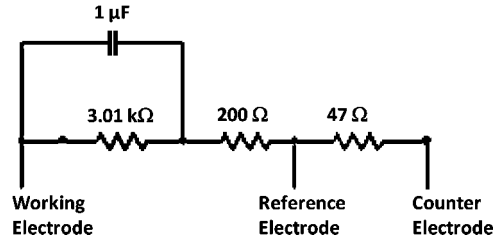

Figure 1. Schematic of the Randles circuit provided by Gamry.

The input impedance of the HT-EIS apparatus was evaluated using a series of open-lead experiments and a previously described procedure.[20] Briefly, the electrode cables for four cells corresponding to a row of cells within the HT-EIS system were connected to Randles circuits to define the open circuit potential (0 ± 3 mV). Then, the experiments were paused; the Randles circuits were removed from the electrode cables, and EIS spectra were recorded simultaneously under an open-lead condition.

Validation Experiment Based on the Redox Couple K_4FeCN_6/K_3FeCN_6. Titanium panels were degreased in acetone, rinsed with distilled water, and then placed in an acid pickling solution (an aqueous solution containing 14 wt % HNO_3 and 1 wt % HF) for 1−3 min until the surface was uniformly white. The panels were then washed with distilled water three times and allowed to air dry.[21] The pretreated titanium substrates were used as working electrodes, and an equal molar (5/5 mM) solution of the redox couple, K_4FeCN_6/K_3FeCN_6, in 0.5 M aqueous $KClO_4$ was used as the electrolyte. The frequency range used was 10^4−0.01 Hz.

Validation Experiments Utilizing a Uniform Polymer Film. Following a procedure previously described,[22] pieces of Tedlar film were coated uniformly with a thin layer of silver-containing epoxy adhesive, and the films were adhered to specimens of AA 2024-T3 to establish a conductive bond between the film and the metal. The AA 2024-T3 specimens laminated with Tedlar film were used as working electrodes for the HT-EIS validation experiment. The electrolyte used in this experiment was 3% NaCl. The frequency range was 10^4−0.01 Hz.

Validation Experiments Utilizing Polymer Coatings. Coatings were applied by spraying coating formulations onto AA 2024-T3 panels using a high-volume/low-pressure spray gun.[23] Coating specimens consisting of a single coating were allowed to cure for at least one week at room temperature before they were tested, and the coating thickness was ∼50 ± 10 μm for all specimens. For the coating system consisting of the Mg-rich primer and polyurethane topcoat, the Mg-rich primer was allowed to cure for one week before the polyurethane topcoat was applied. The average film thickness for specimens based on this coating system was approximately 100 ± 10 μm. The electrolyte for EIS experiments was dilute Harrison's solution (an aqueous solution comprising 0.35% $(NH_4)_2SO_4$ and 0.05% NaCl). The frequency range used was 10^4−0.1 Hz.

Results and Discussion

HT-EIS Apparatus. The basic components of the HT-EIS apparatus are illustrated in Figure 2. An automated

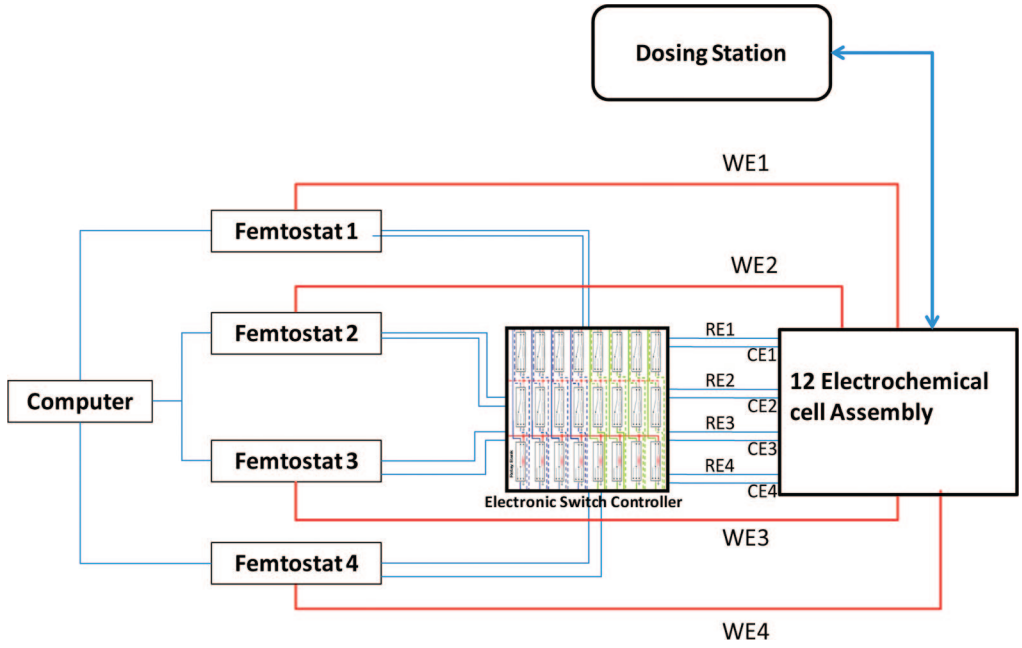

Figure 2. Schematic illustrating the basic components of the HT-EIS system.

electronic switch controller and a 12-unit array of electrochemical cells were fabricated and interfaced with each other. Four femtostats of a Gamry MultiEchem 8 Electrochemical Workstation are connected to the electronic switching system so that four electrochemical measurements can be run simultaneously. The electrochemical measurements are controlled by a computer with Gamry Framework software. A fluid-dosing station is used to control electrolyte delivery and extraction within each cell of the 12-cell electrode assembly.

As shown in Figure 3A, the working electrodes of the 12-cell electrode array are formed using a 20 cm × 10 cm × 0.16 cm piece of metal substrate machined to create four 10 cm × 3.5 cm × 0.16 cm tabs. The tabs can be simultaneously coated using a parallel dip coating process, illustrated in Figure 4, to produce an array of four coatings. The coating array is then bonded to a 20 cm × 10 cm × 0.32 cm PVC backing plate using an epoxy adhesive. After the substrate is securely adhered to the PVC plate, the four tabs are electrically isolated from one another by cutting the top spine holding them together. As illustrated in Figure 3C, the four circular positions in row A are used for the first set of EIS measurements, followed by row B and then row C.

Images illustrating assembly of the HT-EIS system are shown in Figure 5. The four-tab coating array assembly (Figure 3C) is placed into a recessed area of a nylon block (Figure 5A) designed for precisely positioning the array assembly. A second nylon block is then fastened to the uncoated edge of the coating array assembly using four metal screws. In addition to holding the coating array in place, the four metal screws are used as connection posts for working electrode cables. A digital voltmeter is used to ensure good electrical contact is established between the working electrodes and metal screws. Next, a 6.4 mm thick rubber gasket with 12 circular holes (2.54 cm in diameter) is positioned on top of the coating array assembly using the alignment posts (Figure 5B) to create a water-tight seal for the electrolyte reservoirs. A 4 mm thick nylon block possessing

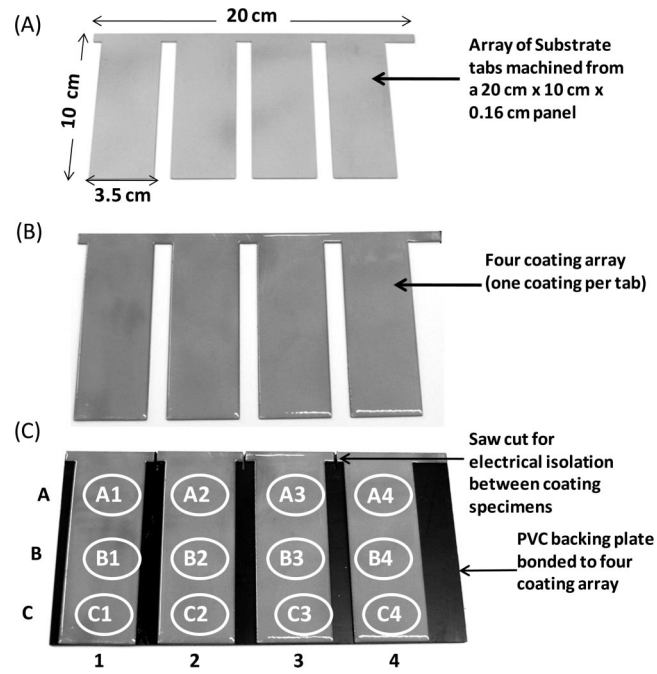

Figure 3. Images showing the four coating array assembly used for the HT-EIS system: the array of substrate tabs machined from a standard panel (A), the four coating array produced by coating each substrate tab (B), and the coating array assembly required for the HT-EIS system (C).

an analogous configuration to the rubber gasket is then placed on top of the rubber gasket and firmly held in place using three stainless steel toggle clamps (Figure 5C) to create 12 electrolyte reservoirs on the surface of the coatings (3 reservoirs per coating). The use of the rubber gasket in conjunction with the clamping device has been shown to eliminate electrolyte leakage. Finally, as shown in Figure 5D, an electrode array assembly is placed on the top of the 12-well assembly to create 12 complete electrochemical cells.

Figure 6 illustrates an individual cell setup within the HT-EIS system. Each cell contains a working electrode (substrate), a Ag/AgCl reference electrode (RE), and a Pt counter

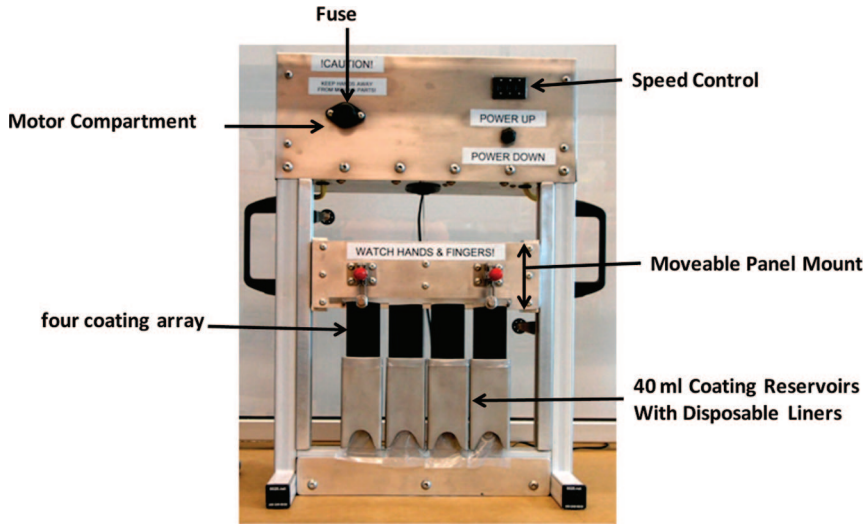

Figure 4. Image of a parallel dip-coater designed for creating a four-tab coating array.

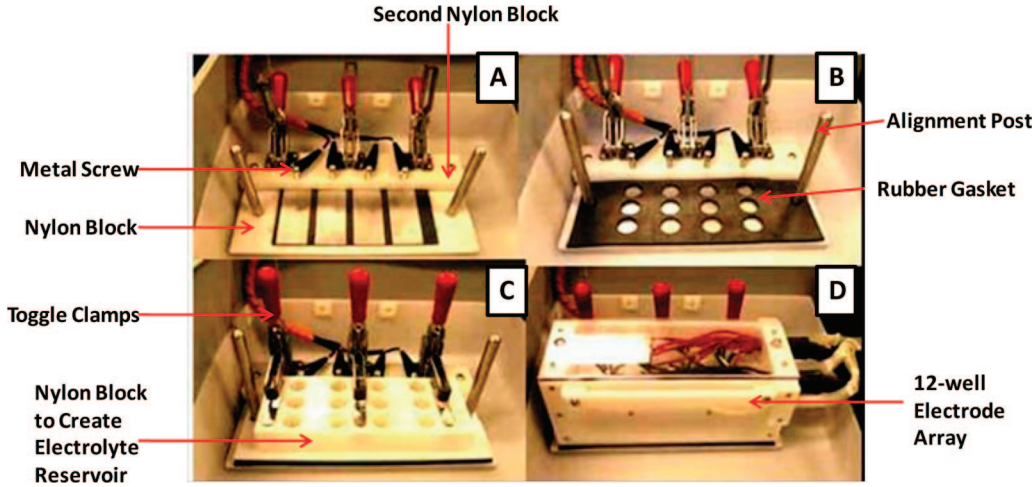

Figure 5. Image displaying the components of the 12-well electrochemical cell assembly: placement of the four coating array assembly (A), placement of the rubber gasket (B), placement and clamping of the nylon block to create the 12-well array of electrolyte reservoirs (C), and placement of the array of electrodes to produce the fully assembled 12-well array of electrochemical cells (D).

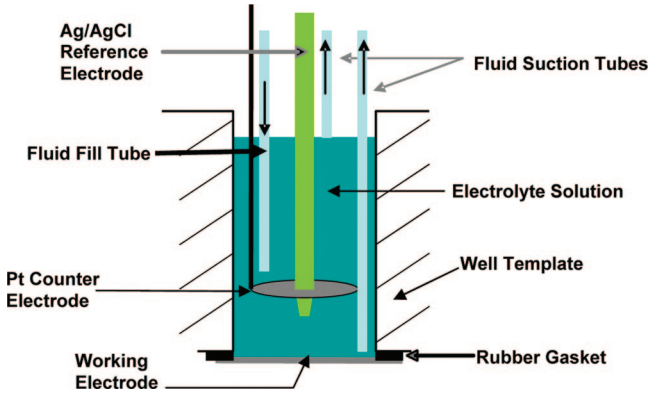

Figure 6. Schematic of an individual cell setup within the HT-EIS system.

electrode (CE). The circular Pt mesh CE (1.2 cm in diameter) was placed about 1.5 cm above the coated metal substrate to form a parallel-planar arrangement with the working electrode. A 5 mm hole was made in the center of the Pt mesh CE to allow insertion of the tip of the reference electrode. The separation distance between the working electrode and RE was adjusted to about 1 cm. To control exposure time of the test specimen to the electrolyte solution, a fluid delivery and extraction system was also incorporated into each cell setup. Electrolyte (10 mL) can be automatically delivered to or extracted from cells simultaneously. The time required to assemble the HT-EIS system starting from placement of the coating array assembly is less than 5 min.

The electronic switch control circuit, shown schematically in Figure 6, was created to perform electrode connection/disconnection operations when changing rows during an experiment. This circuit allows for electrochemical measurements to be conducted simultaneously in groups of four without operator intervention. Row selection is controlled through the control software using the two-channel transistor-transistor logic (TTL) output available on the femtostat. A pair of four-pole mechanical relays is used to convert the two output channels to a four-state binary code decimal allowing for up to four measurement combinations. Two field-effect transistors are used to match the impedance between the relay coils and the TTL outputs. A high quality, shielded coaxial cable is used for all of the signal wiring, and the entire unit is housed in an electro-magnetic interference shielded cabinet. A highly insulated reed relay (Coto Technology, Inc.) is used for the on/off switching of REs

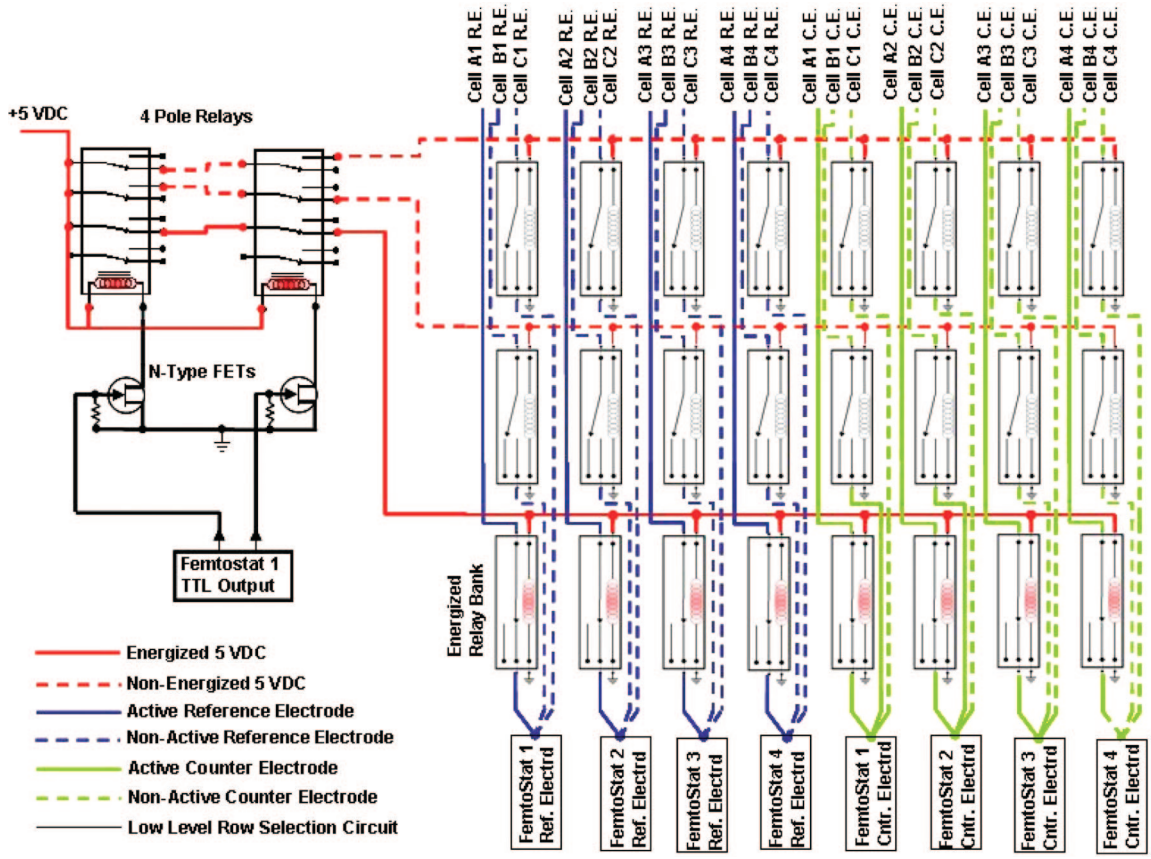

Figure 7. Schematic diagram of the electronic switch control circuit created to perform electrode connection/disconnection operations when changing rows during an experiment. This circuit allows for electrochemical measurements to be conducted simultaneously in groups of four without operator intervention.

and CEs. The working electrodes were simply wired directly to the femtostat input.

Validation of the HT-EIS System. Randles Equivalent Circuit Calibration and Open-Lead Experiment. To test the performance of the HT-EIS system, especially the compatibility of the electronic switching system with the commercial Gamry potentiostat, four identical Randles circuits were used for calibration (Figure 1). Because the EIS spectrum generated from the circuits has a known response, any deviation from the response indicates an issue with instrument operation. Figure 8A displays the 12 Bode plots generated from the respective cells within the HT-EIS system. The 12 plots overlap and the relative standard deviation was less than 0.3% over the entire frequency range, showing very good between-cell reproducibility. The 12 HT-EIS spectra were compared with a theoretical Bode plot, which was calculated using the circuit model and input parameters displayed in Figure 1. As shown in Figure 8B, an excellent correlation ($R^2 = 1$) between the theoretical result and the 12 HT-EIS spectra was obtained indicating that the HT-EIS system can generate highly accurate data over this impedance range.

Open-lead EIS experiments were conducted to evaluate the practical impedance limit of the HT-EIS system such as maximum measurable impedance and lowest measurable capacitance. For this experiment, four cells of the same row of the 12-well electrode array were measured simultaneously and the resulting 12 EIS spectra were numerically simulated using a parallel RC equivalent circuit. The open lead EIS for the Gamry potentiostats (without using the HT-EIS system) were also conducted as a control experiment. As shown in Figure 9, the maximum measurable impedance for the commercial potentiostat was on the order of 3×10^{12} Ω, and the lowest measurable capacitance was about 3.0 ± 1 pF. In contrast, the maximum impedance recorded with the HT-EIS system was about 3×10^{11} Ω, 1 order of magnitude lower than that obtained from the potentiostat. The corresponding lowest capacitance was 30 ± 1.2 pF, which is 1 order of magnitude higher than that obtained from the potentiostat. The lower input impedance of the HT-EIS system was caused by the additional circuitry associated with the electronic switching system and cell cabling associated with the parallel multiplexer, making the DC background current larger than the measured AC signal at extremely high impedance. The test for the minimum impedance limit of the HT-EIS system was not conducted since it is not of interest for coating research.

Validation Experiment Based on the Redox Couple K_4FeCN_6/K_3FeCN_6. A titanium substrate in a redox couple solution, K_4FeCN_6/K_3FeCN_6, was used as a model system to validate the performance of the 12-well array of the HT-EIS system. There were several reasons for choosing this model system for instrument validation. First, titanium, which is a relatively inert metal, generally exhibits good chemical and electrochemical stability when immersed in an electrolyte.[24] Second, neither K_4FeCN_6 nor K_3FeCN_6 show significant adsorption on to titanium surfaces[25] which enables

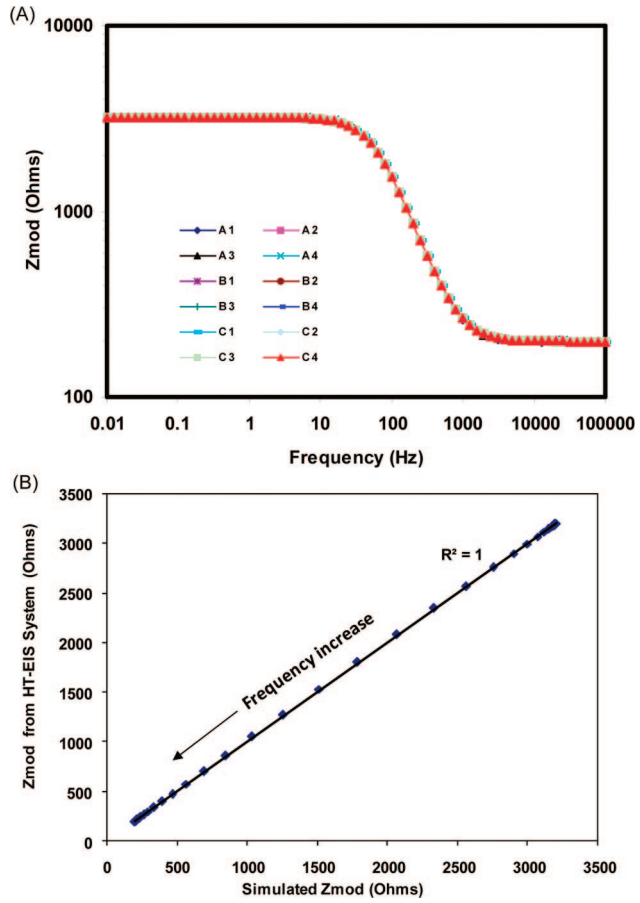

Figure 8. Bode plots generated from each of the 12 electrochemical cells within the HT-EIS system using identical Randles circuits (A). The correlation between impedance modulus generated using the HT-EIS system and the theoretical response obtained using the circuit model and input parameters (B).

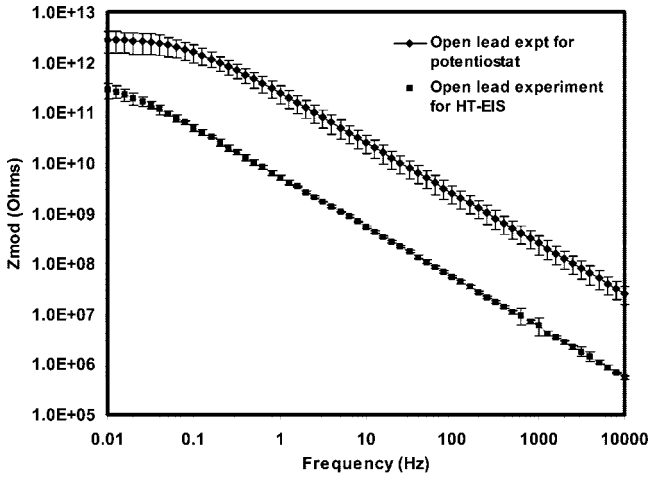

Figure 9. Bode plots obtained from an open lead experiment for the Gamry potentiostat and HT-EIS system.

higher reproducibility for EIS measurements. Further, titanium is physically robust, relatively inexpensive, and easy to handle.

For the validation experiment, a four-tab array (Figure 3A) was machined from a titanium panel. The open circuit potential (OCP) of the metal in the K_4FeCN_6/K_3FeCN_6 electrolyte reached steady state in a few seconds generating a relatively stable value at 0.22 ± 0.02 V vs the Ag/AgCl RE. The OCPs for the four cells comprising a single row of the HT-EIS system were recorded simultaneously and EIS experiments were conducted. As shown in Figure 10A, the 12 Bode plots generated from the experiment were essentially the same, indicating equivalence of each of the 12 electrochemical cells. These results were also compared with results obtained using a conventional, single-cell EIS setup. A good linear correlation ($R^2 = 0.99$) was found over the entire frequency range (Figure 10B) suggesting that the HT-EIS system can provide the same level of data accuracy as a conventional, single-cell EIS setup. The EIS data for both experimental arrangements were fitted using the following equivalent circuit model:

where R1, R2, and CPE are solution resistance, charge transfer resistance, and a constant phase element, respectively. The CPE is used to simulate the surface capacitance effect that compensates for surface heterogeneity in the system. The values obtained for these parameters are listed in Table 1. No significant difference was found between the values obtained with the conventional, single-cell EIS and the values obtained with the HT-EIS system.

Validation Experiments Utilizing a Uniform Polymer Film. In practice, coatings for corrosion protection typically involve high impedances, in the range of 10^9 Ω or higher. Thus, the performance of the HT-EIS system needed to be evaluated further in this high impedance range. Recently, Bierwagen et al.[22] proposed a method for calibrating a potentiostat that involved the use of a commercially available polymer film possessing uniform thickness and little or no film defects. The method is relatively simple, low-cost, and, more importantly, capable of providing highly reproducible results in the high impedance range.

As a result, a Tedlar film of uniform thickness was adhered to AA 2024-T3 and EIS measurements made. As shown in Figure 11A, Bode plots obtained using the HT-EIS system for this film were characteristic of a high-performance coating with very low permeability. The film behaved like a capacitor, generating a straight-line Bode plot with a slope of about −1 and very high impedance (more than 10^{10} Ω) at low frequency.[22] The relative standard deviation (RSD) with respect to the variation in impedance generated from the 12 cells of the HT-EIS system was determined to be 12−19% which was somewhat higher than the 7−15% RSD obtained using 12 replicate measurements made with a conventional, single-cell EIS setup. As shown in Figure 11B, the average impedance values obtained using the HT-EIS system were compared with those obtained using a conventional, single-cell EIS and a good linear correlation ($R^2 = 0.99$) was found between the two set-ups. This results shows that the HT-EIS system is capable of characterizing materials possessing a high, low-frequency impedance. In addition, a CPE circuit model was used to simulate the results generated from the HT-EIS system, and the film capacitance was determined to be 0.64 ± 0.12 nF. From the capacitance, the dielectric constant of the film was calculated and determined

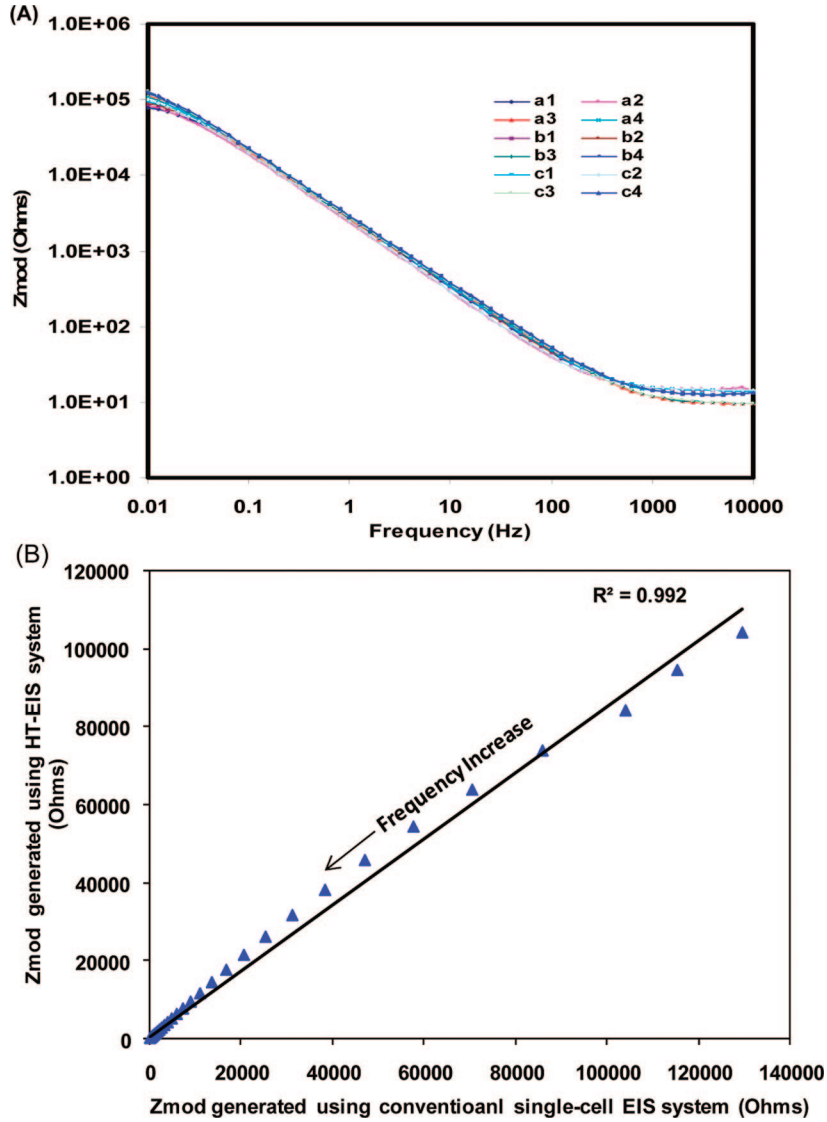

Figure 10. Bode plots generated for the K_4FeCN_6/K_3FeCN_6 redox couple using the HT-EIS system (A). A correlation between impedance moduli generated using the HT-EIS system and those generated with a conventional single-cell EIS setup (B).

Table 1. Electrochemical Parameters Calculated for the Redox Couple K_4FeCN_6/K_3FeCN_6 Using Both the HT-EIS System and a Conventional Single-Cell EIS System

	R_1 (Ω)	R_2 ($\times 10^5$ Ω)	capacitance ($\times 10^{-6}$ F)
single-cell EIS	12.1 ± 2.1	1.31 ± 0.19	73.7 ± 1.6
HT-EIS	11.8 ± 3.8	1.04 ± 0.18	78.5 ± 2.79

to be 7.3. [22] This dielectric constant was within the 5−8 range provided in the technical data sheet for the film.

Validation Experiments Utilizing Polymer Coatings. To test the feasibility of the HT-EIS system for characterization of organic coating systems, a commercial polyurethane coating was applied to the four-tab array derived from a panel of AA 2024-T3. After the panels were cured, scribes were made on all specimens in row C of the array. EIS measurements were performed using all 12 positions of the four specimen array. As shown in Figure 12, the low-frequency impedance obtained for the 8 replicate unscribed samples (rows A and B of the four tab array) varied in the range of 10^6-10^7 Ω, and the coating capacitance ranged between 5.28 and 21.6 nF. These parameters were obtained by fitting the data to a parallel *R*(CPE) equivalent circuit model. This level of variation was higher than that obtained from the model film validation experiment which may be caused by variations in coating thickness and the presence of film defects.

For the scribed positions (row C of the four tab array), the low-frequency impedance values were 2 orders of magnitude lower than for the unscribed positions. The EIS measurements on the four scribed positions produced similar and, in some cases, overlapping spectra. Variations in the manually produced scribes most likely contributed to the variation observed in the Bode plots of the scribed positions.

In addition to using the three positions of a coated specimen for obtaining replicate EIS data, the HT-EIS system can be used to conduct different electrochemical measurements on the same coating specimen to obtain a wide range of information. To illustrate, four different coatings were prepared and applied to AA 2024-T3 using the array format (Figure 13A). The coatings prepared included a chromate-containing epoxy primer (Cr-epoxy), a Mg-rich epoxy primer, a polyurethane primer (MIL-PRF-85285D), and a coating system labeled as Mg/PUR, which is composed of a Mg-rich epoxy primer and a polyurethane topcoat (MIL-PRF-

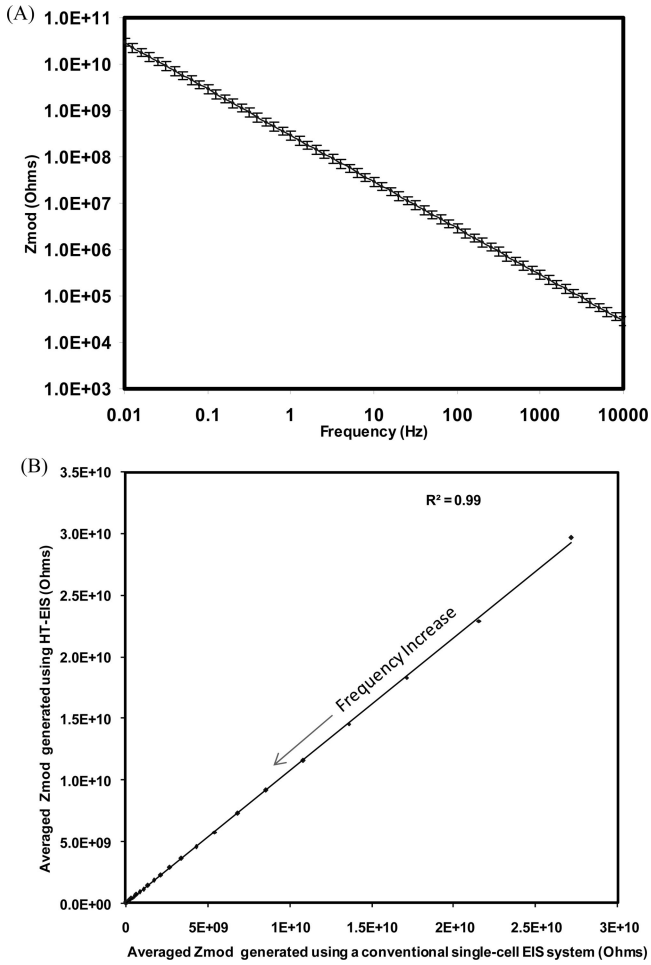

Figure 11. Bode plots for Tedlar film laminated to Al 2024-T3 generated using the HT-EIS system (A). A correlation between impedance moduli generated using the HT-EIS system and those generated with a conventional single-cell EIS setup (B).

85285D). In the top row of the array (row A in Figure 13A), EIS experiments were performed to determine the barrier properties of the coatings. In the middle positions of the array (row B in Figure 13A), linear polarization experiments were conducted to obtain electrochemical parameters such as corrosion current and corrosion potential. Scribes were made in the bottom positions of the coating array (row C in Figure 13A), and EIS was used to characterize the metal-coating interaction in the electrolyte. Utilization of multiple experiments per coating specimen enabled the generation of a plethora of information with the HT-EIS system. For example, the data obtained from the experiment provide the following information:

1. On the basis of Bode plots (Figure 13B) generated using EIS experiments at row A of the coating array, the Cr-epoxy coating was shown to possess the highest low-frequency impedance value (3×10^7 Ω), followed by the top-coated Mg-rich primer, the polyurethane primer, and the Mg-rich primer. The high impedance at low-frequency range for the Cr-epoxy sample (A1) is the result of the known inhibitive properties of chromate pigments by virtue of passivating the metal surface and enhancing or stabilizing the oxide layer at the metal surface. The low impedance value of the Mg-rich primer is attributed to the electrically conductive nature of the coating. The reason that the low frequency impedance for the topcoated Mg-rich primer is higher than that for the polyurethane primer may caused by the film thickness difference between the two forms of coatings. On the other hand, the shape and profile of the Bode plots at higher frequency range (typically from 10 to 10^4 Hz) indicate the capacitive behavior of these coatings. Qualitatively, the capacitances (C) for the four samples can be ranked in the following order: $C_{\text{Mg-richprimer}} > C_{\text{Mg/PUR}} > C_{\text{polyurethane}} > C_{\text{Cr-epoxy}}$. The higher capacitance value suggests the higher content of water ingressing into the coating. The high capacitance for the Mg containing coatings may be attributed to the relative hydrophilic nature of the coating.

2. Corrosion currents measured using linear polarization experiments (Figure 13C) at row B of the coating array showed that the relative ranking of corrosion current was $I_{\text{Cr-epoxy}} < I_{\text{Mg/PUR}} \leq I_{\text{polyurethane}} < I_{\text{Mg-richprimer}}$. It is found that a significant current drop exists between Mg-rich primer and the rest of coatings, which is because the Mg-rich primer offers higher electrical conductivity than the other coatings. The corrosion current ranking was reversely correlated with the low frequency impedance ranking obtained from the EIS measurement at row A of the coating array (Figure 13B). The corrosion potential (−1.2 V vs reference) measured for the Mg-rich primer (Figure 13C) was significantly lower than those for the other coatings and consistent with a mixed potential between Mg and AA 2024-T3. This result, in conjunction with the low impedance (Figure 13B) and high corrosion current observed for the Mg-rich primer, indicates galvanic coupling between Mg particles in the Mg-rich primer and the AA 2024-T3 substrate.

3. Comparing Figure 13B to Figure 13D, one can seen that the introduction of a scribe into the Mg-rich primer-coated sample did not result in a significant reduction in impedance. This result indicates that the primer provides corrosion protection mainly through electrochemical interaction with the substrate. In contrast, the low-frequency impedance for the rest of the coatings decreased significantly after the introduction of the scribes. It is interesting to note that the impedance value for the Cr-epoxy (C1) was still the highest of the four coatings even after introduction of the scratch, the effect of which may be the result of the healing effect established either by the inhibitive pigments leached from the coating[26–31] or by a resistive corrosion product produced by the inhibitive pigments.[32,33] Since looking for corrosion protection mechanisms of these particular coatings is not the main concern of the study, the subject will not be explored in further detail here.

Conclusions

A HT-EIS system based on a four-coating array was developed that enables 12 electrochemical measurements to be made with a minimum of manual intervention. In addition, the system allows for quick assembly when compared to the setup of an equivalent number of single-cell EIS assemblies. It was estimated that the HT-EIS system enables at least a 4-fold reduction in setup time compared to the use of conventional EIS equipment.

System validation experiments comparing results obtained with the HT-EIS system to results obtained using a single-

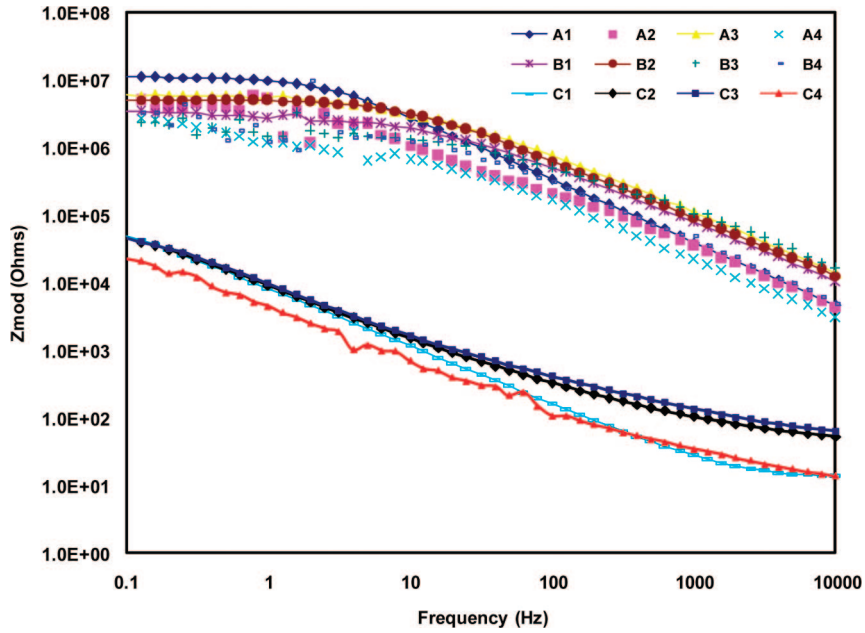

Figure 12. Bode plots for a polyurethane coating on Al 2024-T3 generated using the HT-EIS system. Positions A1−A4 and B1−B4 were not scribed, while positions C1−C4 were scribed prior to making measurements.

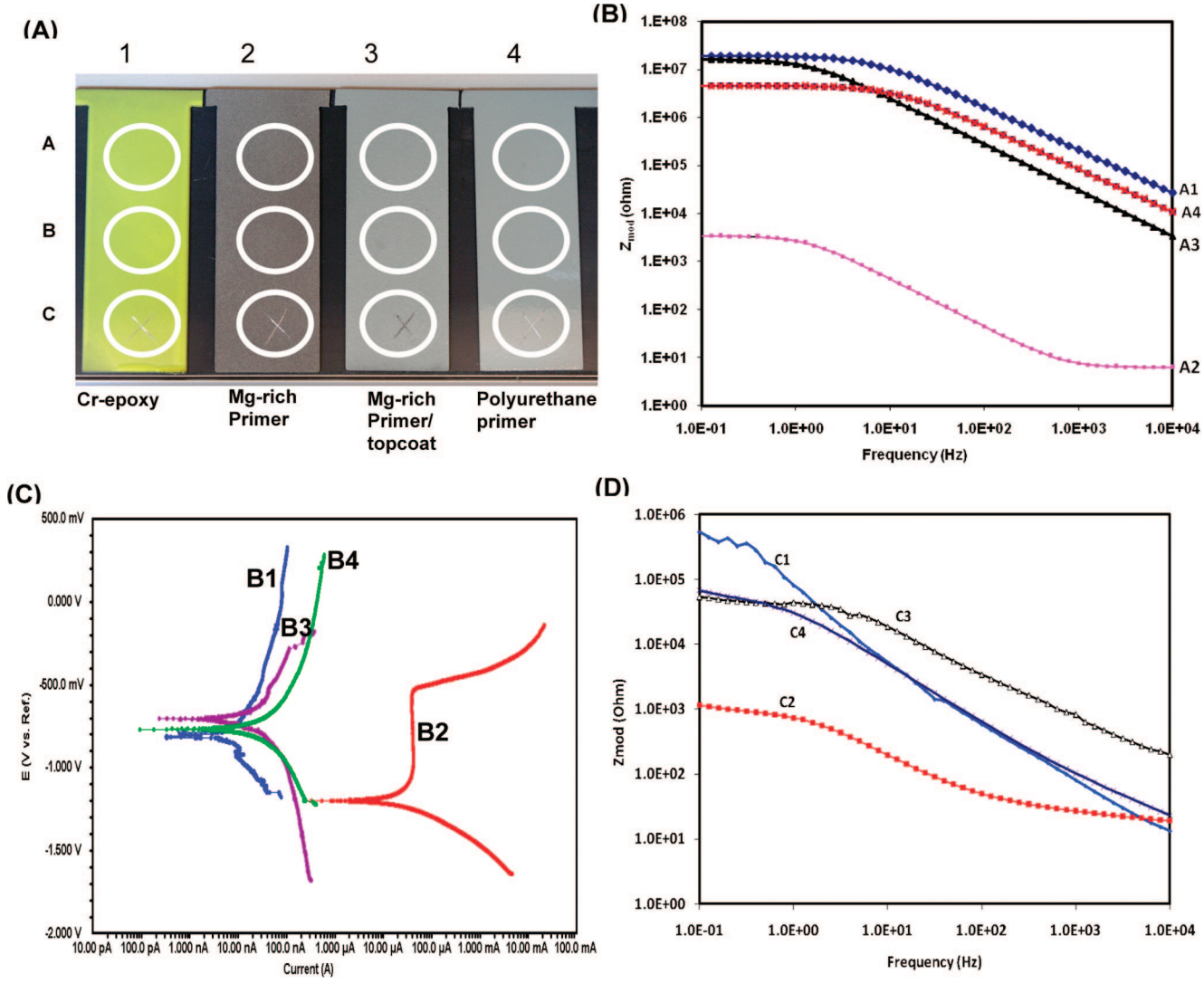

Figure 13. An illustration of the utility of using the HT-EIS system to conduct a variety of electrochemical measurements on the same sample specimen: an image of the four coating array assembly (A), Bode plots generated using row A of the coating array (B), linear polarization measurements using row B of the coating array (C), and Bode plots generated using row C of the coating array (D).

cell EIS assembly indicated that high quality data can be obtained using the HT-EIS system. The maximum impedance and the lowest capacitance that can be measured using the HT-EIS system was determined to be 3×10^{11} Ω and 30 ± 1.2 pF, respectively. The HT-EIS system is currently being used within a full combinatorial workflow designed to enhance the rate of organic coating development.[13,34] The throughput of the system could be further improved by increasing the density of the microelectrode array (e.g., 24-electrode array) and by developing more efficient software to facilitate library design and data analysis.

Acknowledgment. The authors gratefully acknowledge financial support from the Air Force Research Laboratory under Grant FA8650-04-1-5045.

References and Notes

(1) *Corrosion Cost and Preventive Strategies in the United States*; CC Technologies Laboratories: Dublin, OH 2001.
(2) Wranglen, G. *An Introduction to Corrosion and Protection of Metals*; Institute for Metallurgy: Stockholm, Sweden, 1972.
(3) Grundmeier, G.; Schmidt, W.; Stratmann, M. *Electrochim. Acta* **2000**, *45*, 2515–2533.
(4) Rammelt, U.; Reinhard, G. *Prog. Org. Coat.* **1992**, *21*, 205–226.
(5) Van Westing, E. P. M.; Ferrari, G. M.; De Wit, J. H. W. *Electrochim. Acta* **1994**, *39*, 969–973.
(6) *Standard Practice for Operating Salt Spray (Fog) Apparatus*; ASTM B117−97; ASTM International: West Conshohocken, PA, 1996.
(7) *Standard Practice for Cyclic Salt Fog/UV Exposure of Painted Metal*; ASTM D5894−96; ASTM International: West Conshohocken, PA, 1996.
(8) Cawse, J. N.; Olson, D.; Chisholm, B. J.; Brennan, M.; Sun, T.; Flanagan, W.; Akhave, J.; Mehrabi, A.; Saunders, D. *Prog. Org. Coat.* **2003**, *47*, 128–135.
(9) Chisholm, B.; Potyrailo, R.; Cawse, J.; Shaffer, R.; Brennan, M.; Molaison, C.; Whisenhunt, D.; Flanagan, B.; Olson, D.; Akhave, J.; Saunders, D.; Mehrabi, A.; Licon, M. *Prog. Org. Coat.* **2002**, *45*, 313–321.
(10) Chisholm, B.; Potyrailo, R.; Shaffer, R.; Cawse, J.; Brennan, M.; Molaison, C. *Progress in Organic Coatings* **2003**, *48*, 219–226.
(11) Chisholm, B.; Potyrailo, R.; Shaffer, R.; Cawse, J.; Brennan, M.; Molaison, C. *Prog. Org. Coat.* **2003**, *47*, 112–119.
(12) Chisholm, B. J.; Potyrailo, R. A.; Cawse, J. N.; Shaffer, R. E.; Brennan, M.; Molaison, C. A. *Prog. Org. Coat.* **2003**, *47*, 120–127.
(13) Webster, D. C.; Chisholm, B. J.; Stafslien, S. J. *Biofouling* **2007**, *23*, 179–192.
(14) Jayaraman, S.; Baeck, S.-H.; Jaramillo, T. F.; Kleiman-Shwarsctein, A.; McFarland, E. W. *Rev. Sci. Instrum.* **2005**, *76*, 1–5.
(15) Baeck, S. H.; Jaramillo, T. F.; Brandli, C.; McFarland, E. W. *J. Comb. Chem.* **2002**, *4*, 563–568.
(16) Guerin, S.; Hayden, B. E.; Lee, C. E.; Mormiche, C.; Owen, J. R.; Russell, A. E.; Theobald, B.; Thompsett, D. *J. Comb. Chem.* **2004**, *6*, 149–158.
(17) Fleischauer, M. D.; Hatchard, T. D.; Rockwell, G. P.; Topple, J. M.; Trussler, S.; Jericho, S. K.; Jericho, M. H.; Dahn, J. R. *J. Electrochem. Soc.* **2003**, *150*, A1465−A1469.
(18) Reddington, E.; Sapienza, A.; Gurau, B.; Viswanathan, R.; Sarangapani, S.; Smotkin, E. S.; Mallouk, T. E. *Science* **1998**, *280*, 1735–1737.
(19) Randles, J. E *Discuss. Faraday Soc.* **1947**, *1*, 11.
(20) Loveday, D.; Peterson, P.; Rodgers, B. *JCT Coat. Technol.* **2004**, *1*, 46–52.
(21) *Standard Guide for Descaling and Cleaning Titanium and Titanium Alloy Surfaces*; ASTM B 600−91; ASTM International, Inc.: West Conshohocken, PA, 1991.
(22) Bonitz, V. S.; Hinderliter, B. R.; Bierwagen, G. P. *Electrochim. Acta* **2006**, *51*, 3558–3565.
(23) Fact Sheet: High Volume Low Pressure Spray Equipment; Wisconsin Department of Natural Resources, 1993.
(24) Hurlen, T.; Wilhelmsen, W. *Electrochim. Acta* **1986**, *31*, 1139–1146.
(25) Hurlen, T.; Wilhelmsen, W. *Electrochim. Acta* **1988**, *33*, 1729–1733.
(26) Suda, A. *Hyomen Kagaku* **2001**, *22*, 136–143.
(27) Zhao, J.; McCreery, R. L.; Frankel, G. S.; Allen, F. *Abstr. Pap.—Am. Chem. Soc.* **2000**, *220th*, ANYL-163.
(28) Ramsey, J. D.; McCreery, R. L. *J. Electrochem. Soc.* **1999**, *146*, 4076–4081.
(29) Zhao, J.; Frankel, G.; McCreery, R. L. *J. Electrochem. Soc.* **1998**, *145*, 2258–2264.
(30) Suda, A.; Asari, M. *Zairyo to Kankyo* **1997**, *46*, 95–102.
(31) Lu, Y.; Ren, Y.; Ying, H.; Wu, J.; Zhang, P.; Meng, H. *Proc. Int. Conf. Surf. Sci. Eng.* **1995**, 205–208.
(32) Lohrengel, M. M. *Mater. Sci. Eng., R: Rep.* **1993**, *R11*, 243–294.
(33) Schmitt, G.; Schultze, J. W.; Fassbender, F.; Buss, G.; Luth, H.; Schoning, M. *J. Electrochim. Acta* **1999**, *44*, 3865–3883.
(34) Chisholm, B. J.; Webster, D. C. *J. Coat. Technol. Res* **2007**, *4*, 1–12.

CC8000458